Appl. Phys. A (2016) 122:531
DOI 10.1007/s00339-016-0077-9

Applied Physics A
Materials Science & Processing

Strain effect on ferroelectric polarization of epitaxial $LuFeO_3$ thin films

Yoonho Ahn[1] · Joonkyung Jang[2] · Jong Yeog Son[1]

Received: 24 February 2016 / Accepted: 15 April 2016 / Published online: 27 April 2016

Abstract Epitaxial $LuFeO_3$(LFO) thin films were deposited on $La_{0.5}Sr_{0.5}MnO_3$(LSMO)/$LaAlO_3$(LAO) substrates by pulsed laser deposition method. The LFO thin film with a thickness of 100 nm exhibited tetragonally strained structure on the LSMO/LAO substrate, in which the film showed *c*/*a* ratio of 1.045 based on X-ray diffraction experiment. The LFO thin film had a remnant polarization of about 15.2 μC/cm^2, which was higher than the previously reported values. By using piezoresponse force microscopy study, it was confirmed that the LFO thin films had mosaic ferroelectric domain structure and that their domain wall energy was estimated to be lower than that of $PbTiO_3$ thin films.

1 Introduction

Ferroelectric materials have shown significant abilities for applications such as nonvolatile random access memories, electronic devices, and energy harvesting devices due to their ferroelectricity, piezoelectricity, and pyroelectricity [1–6]. Particularly, Pb(Zr,Ti)O_3 (PZT) materials have attracted considerable attention because of their high remnant polarizations and piezoelectric coefficients [7, 8]. Nevertheless, PZT materials have some problems such as polarization fatigue and toxicity due to lead component. In the case of fatigue problem in PZT materials, it could be overcome by using oxide electrodes such as IrO_2 and RuO_2 [9, 10]. On the other hand, because their toxicity is deadly to our environment and human body, we need to develop lead-free ferroelectric materials and replace PZT materials with them [11–13].

A variety of perovskite-structured materials including $BaTiO_3$ (BTO), $BiFeO_3$ (BFO), $K_{0.5}Na_{0.5}NbO_3$ (KNN), and $Na_{0.5}Bi_{0.5}TiO_3$ (NBT) have been known as lead-free ferroelectrics [11, 12]. However, most of them have low ferroelectric polarizations and piezoelectric coefficients compared to PZT materials [11]. Therefore, we need to improve these physical properties of lead-free ferroelectric materials. In this respect, by controlling the strain between thin film and substrate (or bottom electrode), it is possible to maximize the remnant polarization in ferroelectrics [14]. It has been reported that the strain effects resulted from optimum lattice misfit by using proper bottom electrodes led to the enhanced ferroelectric polarizations [14–16]. Recently, tetragonal BFO thin films exhibited the enhanced ferroelectric polarizations compared to those of PZT thin films by using the $La_{0.5}Sr_{0.5}MnO_3$(LSMO)/$LaAlO_3$(LAO) substrates [17, 18].

In this work, we investigated the enhanced ferroelectric properties of epitaxial $LuFeO_3$ (LFO) thin films deposited on LSMO/LAO substrates by pulsed laser deposition method. The LFO, which is one of the rare-earth orthoferrites, has been considered to be potential multiferroics [19, 20]. Nevertheless, it has been reported that the LFO thin films showed very low ferroelectric polarizations [20–22]. We confirmed that a 100-nm-thick LFO thin film showed the tetragonally strained structure with a *c*/*a* ratio of 1.045 and the enhanced ferroelectric polarization with a

✉ Yoonho Ahn
yahn@khu.ac.kr

✉ Jong Yeog Son
jyson@khu.ac.kr

[1] Department of Applied Physics and Institute of Natural Sciences, Kyung Hee University, Yongin 446-701, South Korea

[2] Department of Nanoenergy Engineering, Pusan National University, Busan 609-735, South Korea

high remnant polarization of 15.2 μC/cm^2. The LFO thin films exhibited mosaic domain structure, and their ferroelectric domain wall energy was lower than that of PZT thin films.

2 Experimental details

Epitaxial LFO thin films were deposited on LSMO/LAO substrates by pulsed laser deposition (PLD) method. LFO target prepared by conventional solid-state reaction method was used for epitaxial thin-film deposition. A frequency-tripled ($\lambda = 355$ nm) Nd:YAG laser with a power of 2×10^4 J/m^2 at a frequency of 2 Hz was used for the PLD deposition, and the distance between the targets and the substrates was 5 cm. The base pressure was about 1.33×10^{-4} Pa, and the substrate temperature was set to 800 °C under an oxygen pressure of 6.65 Pa. After deposition, LFO thin films were cooled down to room temperature in oxygen ambient at 4.0×10^4 Pa. Pt top electrodes with a diameter of 100 μm and a thickness of 100 nm on the LFO thin films were fabricated to prepare Pt/LFO/LSMO capacitors using RF magnetron sputtering techniques. The electrodes were then annealed at 400 °C for 5 min before measuring the ferroelectric properties using an RT66A (Radiant Technologies, Ins.) test system at 2 kHz. Atomic force microscopy (AFM) and piezoelectric force microscopy (PFM) were used to examine their surface morphology and ferroelectric domain structure, respectively.

3 Results and discussion

We depicted a schematic configuration of the LFO thin film on the LSMO/LAO substrate as shown in Fig. 1a. Since thin-film layer of the LSMO electrode is very thin, the LFO thin film is expected to be strained enough to approach a lattice constant of the LAO substrate. Figure 1b shows $\theta-2\theta$ X-ray diffraction (XRD) patterns of the 100-nm-thick LFO thin film on the LSMO/LAO substrate. The (001) and (002) LFO peaks were observed on (100) LSMO/(100) LAO substrate without any other orientation peaks. Figure 1c shows Φ-scans of (101) peak of the LFO thin film and (101) peak of the LAO substrate. The full width at half maximums (FWHMs) of the (001) and (002) peaks were estimated to be about 0.8° and 0.9°, respectively. In a rocking curve experiment, the exhibited FWHMs of the (001) and (002) peaks were 0.8° and 0.9°, respectively (not shown here). These low FWHMs indicate that the LFO thin

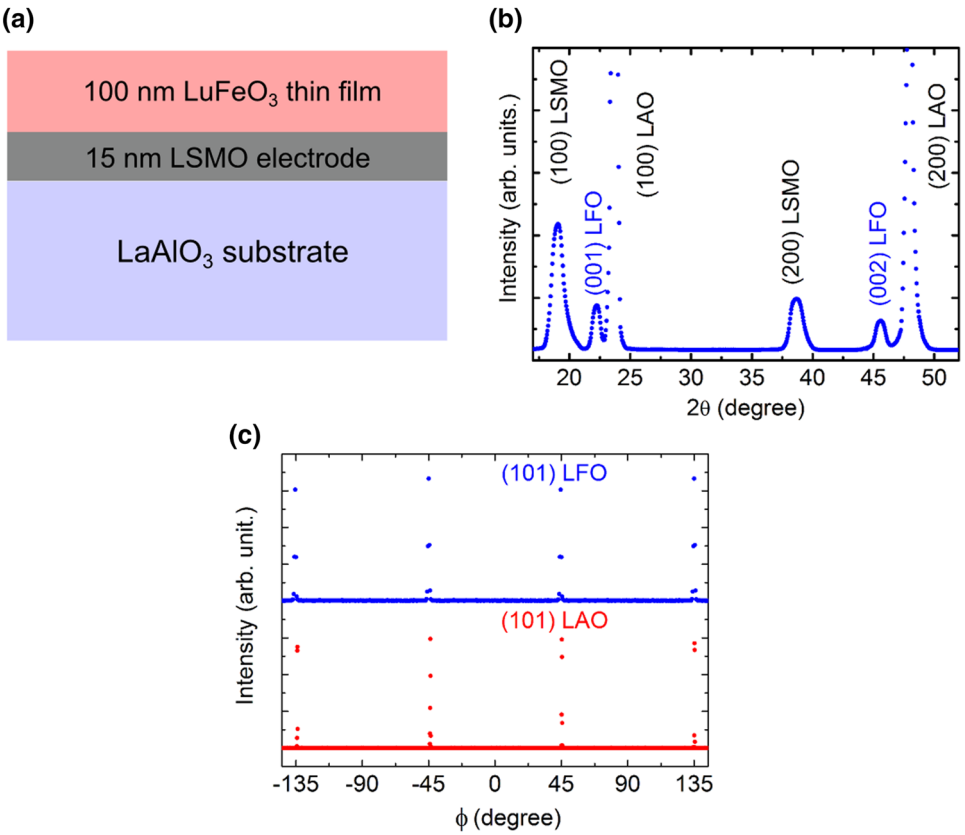

Fig. 1 **a** Schematic drawing of the LFO thin films on LSMO/LAO substrates. **b** $\theta-2\theta$ XRD patterns of the LFO thin film (100 nm), LSMO electrode (15 nm), and LAO substrate. **c** Φ-scans of (101) peaks of the LFO thin film and LAO substrate

film has a good crystallinity along the out-of-plane direction. From the (001) and (002) peaks of the LFO thin film, we obtained the *c*-lattice constant of 3.97 Å.

To confirm in-plane crystallinity of the LFO thin film, we performed the azimuth angle (Φ) scans of the (101) peaks around the *c*-axis. Figure 1c shows the Φ-scans for the (101) LFO thin film and (101) LAO substrate where fourfold symmetry of two in-plane peaks was observed. The concurrence of the peaks means that unit cells of the LFO film and LAO substrate are parallel to each other along the in-plane direction. Thus, we can infer that the LFO thin film have grown heteroepitaxially on the LAO substrate. For the LFO thin film, the FWHM of the rocking curve of (101) peak gave a value of about 0.7°, which indicates the well-defined crystallinity along the in-plane orientation. From the (101) peak, we could estimate the *a*-lattice constant of 3.80 Å. Consequently, it is expected that the relatively high tetragonality (*c*/*a* ratio ∼ 1.045) of LFO thin film caused by the heteroepitaxial growth will induce good ferroelectric properties.

To characterize ferroelectric properties of the epitaxial LFO thin film on the LSMO/LAO substrate, we measured ferroelectric hysteresis loop of the Pt/LFO/LSMO capacitors at a frequency of 2 kHz. Figure 2a shows the ferroelectric polarization–electric field (P–E) curve for the LFO capacitor. The remnant polarization value of the LFO capacitor is about 15.2 μC/m^2, which is much larger than those of the previously reported LFO capacitors [20, 22]. As expected, the epitaxial BTO thin film on the LSMO/LAO substrate exhibited the enhanced ferroelectric polarization. We also obtained a typical piezoelectric hysteresis loop of the LFO thin film by PFM at a measurement frequency of 10 kHz. The hysteresis loop shows a coercive voltage of about 2.0 V and an effective remnant piezoelectric coefficient of about 23 pm/V, respectively, in Fig. 2b.

Figure 3 shows surface morphology and ferroelectric domain structure of the LFO thin film. The window size and scale bar are 150 and 30 nm, respectively. Square-shaped grains are observed on the surface of the LFO thin film as shown in Fig. 3a AFM image. The average grain size of the LFO thin film was estimated to be about 32 nm. The root-mean-square (RMS) surface roughness of the LFO thin film was approximately 5.2 nm. Figure 3b shows the PFM image of the LFO thin film where mosaic ferroelectric domains are observed with clear contrast.

We investigated the correlation between ferroelectric domain size and thickness of the LFO thin film. The well-

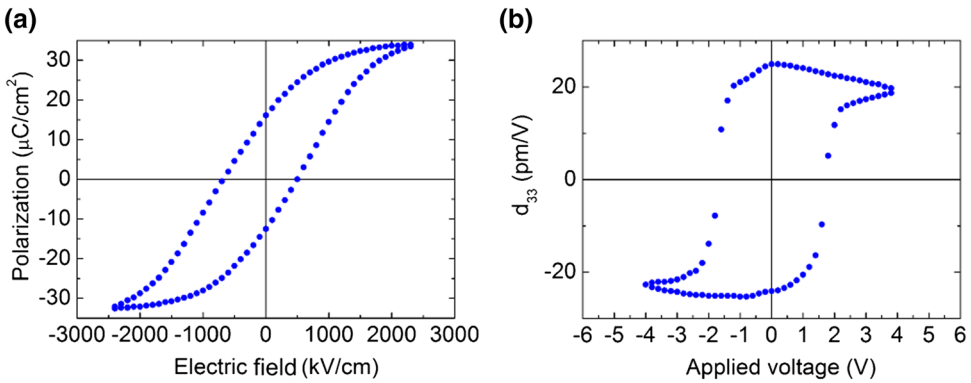

Fig. 2 **a** Ferroelectric hysteresis (P–E) loop of the Pt/LFO/LSMO capacitor. **b** Piezoelectric coefficient (d_{33}) of the LFO thin film is plotted against the applied voltage

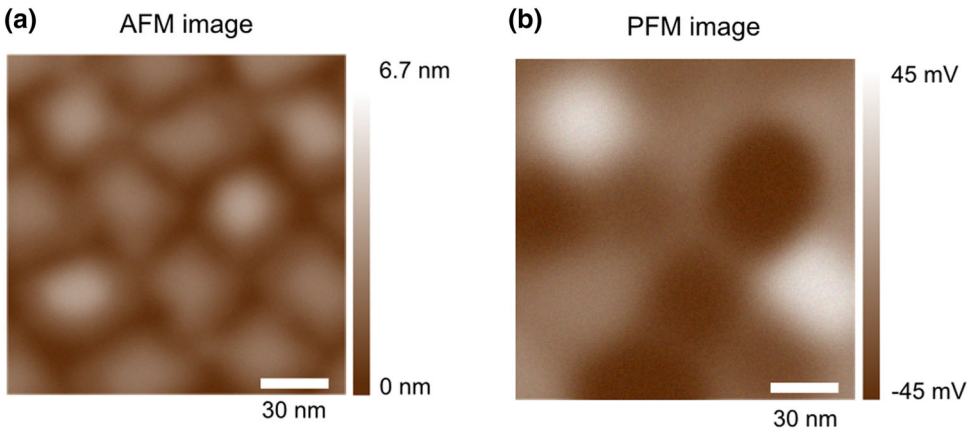

Fig. 3 **a** AFM and **b** PFM images of the LFO thin film

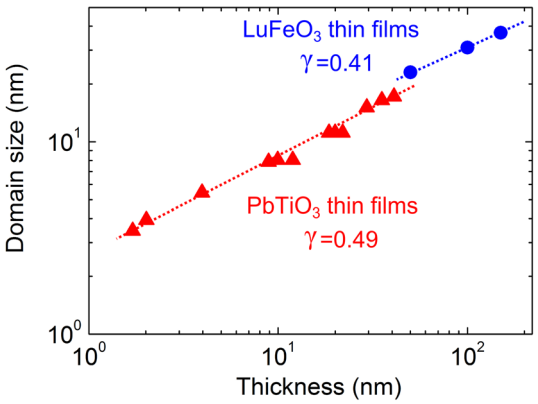

Fig. 4 Domain size as a function of thickness for the LFO and PTO thin films

known Landau-Lifshitz-Kittel (LLK) scaling law has generally been applied to ferromagnetic and ferroelectric domains, in which domain size is proportional to the square root of film thickness ($w = Ad^{\gamma}$, w is the domain width, d is the film thickness, γ is the scaling exponent with the value close to 1/2) [23]. By varying thickness of the LFO films, we plotted the domain sizes as shown in Fig. 4. For comparison, the domain sizes of $PbTiO_3$ (PTO) thin films reported previously were added [24]. Their scaling exponents were determined by least squares fitting. The γ values of LFO and PTO thin films are 0.41 and 0.49, respectively, which means that domain wall energy of the LFO thin films is lower than that of the PTO thin films.

4 Conclusions

In conclusion, we fabricated the strained epitaxial LFO thin films deposited on LSMO/LAO substrates by PLD method. The 100-nm-thick LFO thin film showed tetragonal structure with a *c*/*a* ratio of 1.045 due to strain effect. The LFO thin film exhibited the enhanced remnant polarization of 15 μC/cm^2. It was confirmed that the LFO thin films had mosaic domain structures. From the LLK scaling law, it was inferred that the domain wall energy of LFO thin films was lower than that of PTO thin films.

Acknowledgments This study was supported by the National Research Foundation of Korea (NRF) Grant funded by the Korea government (No. 2015R1A2A2A05027951).

References

1. N. Setter, D. Damjanovic, L. Eng, G. Fox, S. Gevorgian, S. Hong, A. Kingon, H. Kohlstedt, N.Y. Park, G.B. Stephenson, I. Stolitchnov, A.K. Taganstev, D.V. Taylor, T. Yamada, S. Streiffer, J. Appl. Phys. **100**, 051606 (2006)
2. J.F. Scott, Science **315**, 954 (2007)
3. H. Ishiwara, J. Nanosci. Nanotechnol. **12**, 7619 (2012)
4. N. Nuraje, K. Su, Nanoscale **5**, 8752 (2013)
5. C.R. Bowen, H.A. Kim, P.M. Weaver, S. Dunn, Energ. Environ. Sci. **7**, 25 (2014)
6. Y. Yuan, Z. Xiao, B. Yang, J. Huang, J. Mater. Chem. A **2**, 6027 (2014)
7. N. Izyumskaya, Y.I. Alivov, S.J. Cho, H. Morkoç, H. Lee, Y.S. Kang, Crit. Rev. Solid State Mater. Sci. **32**, 111 (2007)
8. P. Muralt, J. Micromech. Microeng. **10**, 136 (2000)
9. T. Nakamura, Y. Nakao, A. Kamisawa, H. Takasu, Appl. Phys. Lett. **65**, 1522 (1994)
10. H.N. Al-Shareef, O. Auciello, A.I. Kingon, J. Appl. Phys. **77**, 2146 (1995)
11. T. Shrout, S. Zhang, J. Electroceram. **19**, 113 (2007)
12. E. Aksel, J.L. Jones, Sensors **10**, 1935 (2010)
13. R.-A. Eichel, H. Kungl, Funct. Mater. Lett. **03**, 1 (2010)
14. D.G. Schlom, L.-Q. Chen, C.-B. Eom, K.M. Rabe, S.K. Streiffer, J.-M. Triscone, Annu. Rev. Mater. Res. **37**, 589 (2007)
15. K.J. Choi, M. Biegalski, Y.L. Li, A. Sharan, J. Schubert, R. Uecker, P. Reiche, Y.B. Chen, X.Q. Pan, V. Gopalan, L.-Q. Chen, D.G. Schlom, C.B. Eom, Science **306**, 1005 (2004)
16. Y. Ahn, J. Seo, J. Jang, J.Y. Son, Mater. Lett. **161**, 168 (2015)
17. J.E. Rault, W. Ren, S. Prosandeev, S. Lisenkov, D. Sando, S. Fusil, M. Bibes, A. Barthelemy, L. Bellaiche, N. Barrett, Phys. Rev. Lett. **109**, 267601 (2012)
18. D. Mazumdar, V. Shelke, M. Iliev, S. Jesse, A. Kumar, S.V. Kalinin, A.P. Baddorf, A. Gupta, Nano Lett. **10**, 2555 (2010)
19. W. Wang, J. Zhao, W. Wang, Z. Gai, N. Balke, M. Chi, H.N. Lee, W. Tian, L. Zhu, X. Cheng, D.J. Keavney, J. Yi, T.Z. Ward, P.C. Snijders, H.M. Christen, W. Wu, J. Shen, X. Xu, Phys. Rev. Lett. **110**, 237601 (2013)
20. U. Chowdhury, S. Goswami, D. Bhattacharya, J. Ghosh, S. Basu, S. Neogi, Appl. Phys. Lett. **105**, 052911 (2014)
21. Y.K. Jeong, J.-H. Lee, S.-J. Ahn, H.M. Jang, Chem. Mater. **24**, 2426 (2012)
22. L. Zhu, H. Deng, J. Liu, L. Sun, P. Yang, A. Jiang, J. Chu, J. Cryst. Growth **387**, 6 (2014)
23. G. Catalan, H. Béa, S. Fusil, M. Bibes, P. Paruch, A. Barthélémy, J.F. Scott, Phys. Rev. Lett. **100**, 027602 (2008)
24. W.-H. Kim, J. Son, Electron. Mater. Lett. **10**, 107 (2014)